Geomechanics and Engineering, *Vol. 31, No. 4 (2022) 409-422*
https://doi.org/10.12989/gae.2022.31.4.409

Sustainable use of OPC-CSA blend for artificial cementation of sand: A dosage optimization study

Sathya Subramanian[1a], Wei Zhong Tee[1b], Juhyuk Moon[2c] and Taeseo Ku*[3]

[1]*Department of Civil and Environmental Engineering, National University of Singapore, 1 Engineering Drive 2, Singapore 117576*
[2]*Department of Civil and Environmental Engineering, Seoul National University, Seoul 08826, South Korea*
[3]*Department of Civil and Environmental Engineering, Konkuk University, 120 Neungdong-ro, Gwangjin-gu, Seoul 05029, South Korea*

(*Received February 23, 2022, Revised June 20, 2022, Accepted August 13, 2022*)

Abstract. The use of calcium sulfoaluminate (CSA) cement as a rapid-hardening cement admixture or eco-friendly alternate for ordinary Portland cement (OPC) has been attempted over the years, but the cost of CSA cement and availability of suitable aluminium resource prevent its wide practical application. To propose an effective ground improvement design in sandy soil, this study aims at blending a certain percentage of CSA with OPC to find an optimum blend that would have fast-setting behavior with a lower carbon footprint than OPC without compromising the mechanical properties of the cemented sand. Compared to the 100% CSA case, initial speed of strength development of blended cement is relatively low as it is mixed with OPC. It is found that 80% OPC and 20% CSA blend has low initial strength but eventually produces equivalent ultimate strength (28 days curing) to that of CSA treated sand. The specific OPC-CSA blend (80:20) exhibits significantly higher strength gain than using pure OPC, thus allowing effective geotechnical designs for sustainable and controlled ground improvement. Further parametric studies were conducted for the blended cement under various curing conditions, cement contents, and curing times. Wet-cured cement treated sand had 33% lower strength than that of dry-cured samples, while the stiffness of wet-cured samples was 25% lower than that of dry-cured samples.

Keywords: blended cement; calcium sulfoaluminate; cement treated sand; ordinary Portland cement; small strain shear modulus

1. Introduction

Ordinary Portland cement (OPC) is a commonly used binding admixture for artificial cementation of soil, which is a ground improvement technique used to enhance the mechanical properties of weak soils (Shooshpasha and Shirvani 2015, Yilmaz *et al.* 2017, Saberian *et al.* 2018, Choi *et al.* 2019, Lee *et al.* 2019). Artificial cementation can have significant influences on the strength (Consoli *et al.* 2012, 2021, Rios *et al.* 2014, Shen *et al.* 2019, Moon *et al.* 2020), compressibility (Horpibulsuk *et al.* 2004), small strain shear modulus (Xiao *et al.* 2018, Yao *et al.* 2018, Khan *et al.* 2019), and seepage (Subramanian *et al.* 2020b) properties of soils. The hydration mechanism and subsequent improvement in the properties of the soil have been well documented. Although extensive research has been carried out over the decades, concerns remain about the carbon dioxide (CO_2) emission during OPC production, as it accounts for about 5% of man-made CO_2 emissions (Trauchessec *et al.* 2015). Hence, there is a need to replace OPC with an eco-friendlier binder without compromising the mechanical properties of improved soil.

One such alternative, eco-friendly binder admixture is calcium sulfoaluminate (CSA) cement. The major constituent of CSA cement is ye'elimite, which releases less CO_2 compared to OPC during its production and has much faster strength development. The conversion of raw minerals to ye'elimite requires a lesser temperature (about 200ºC lower than that of OPC production), and the CO_2 formed as a by-product during the production is also lesser (Winnefeld and Lothenbach 2010, Juenger *et al.* 2011, Pooni *et al.* 2021). With the characteristic of CSA having a lower carbon footprint than OPC, recently, some studies have been carried out to understand the mechanical properties of CSA treated sand for geotechnical application (Subramanian *et al.* 2018, Moon *et al.* 2020). For instance, it is expected CSA cement treated sand exhibits higher initial strength than that of OPC treated sand. CSA cement with optimum gypsum content resulted in rapid formation of ettringite crystal, which led to higher initial strength (Subramanian *et al.* 2019b). Also, several studies have been carried out to examine the performance CSA treated silty sand subjected to freeze-thaw cycle (Jumassultan *et al.* 2021, Sagidullina *et al.* 2022). Although CSA is an eco-friendly cement with higher material performance, the cost of CSA cement is generally higher due to the fact that it relies on a higher aluminum proportion (Trauchessec *et al.* 2015).

*Corresponding author, Associate Professor
E-mail: tsku@konkuk.ac.kr
[a]Research Fellow
E-mail: subramanian@nus.edu.sg
[b]Undergraduate student
[c]Associate Professor
E-mail: juhyukmoon@snu.ac.kr

Copyright © 2022 Techno-Press, Ltd.

ISSN: 2005-307X (Print), 2092-6219 (Online)

In concrete technology, OPC and CSA cements can be blended to combine the advantages of both cement types (Trauchessec *et al.* 2014, 2015, Chaunsali and Mondal 2015, Mehdipour and Khayat 2018, Wolf *et al.* 2019, Huang *et al.* 2021, Park *et al.* 2021). The research on OPC-CSA blended cement for concrete technology is discussed in the next section. Although the cost of CSA cement is relatively high, its use has been actively increasing as a setting controlling admixture and shrinkage-compensating admixture. From a geotechnical standpoint, similarly, it would be advantageous to use the OPC-CSA blend, to lower the initial cost (against using pure CSA) and/or to obtain the characteristic of high strength gain of CSA. However, the use of OPC-CSA blended cement in geotechnical application has not been explored yet, where the required water to cement ratio is higher. As a continuation of the study on CSA cement, this research explores the use of OPC-CSA blended cement for geotechnical application. Therefore, the objective of this research is to find an optimum OPC-CSA blend at higher water to cement ratio conditions that exhibits sustainable strength gain with time at low production cost. Also, this study examines the applicability of OPC-CSA blend under various conditions (e.g., curing time, curing method, and cement content) by quantifying the unconfined compressive strength development of the blended cement treated sands. To support the observed unconfined compressive strength data and also to examine the structural changes of the cemented sand, further investigations were made through bender element testing, scanning electron microscopy (SEM), and X-ray diffraction (XRD) analyses.

1.1 Background

The hydration mechanism of CSA is complicated, as ye'elimite (the major compound in CSA cement) hydration products depend on the amount of sulfate and lime. In the absence of lime, ye'elimite hydrates in presence of sulfate to form ettringite and gibbsite (Eq. (1)), which helps in the high initial strength, while in the absence or less concentration of sulfate it forms monosulfoaluminate and gibbsite (Eq. (2)) (Lan and Glasser 1996, Winnefeld *et al.* 2017). But with the presence of lime and absence of sulfate, ye'elimite hydrates to form monosulfoaluminate-hydroxy solid solution. In presence of both lime and sulfate, ye'elimite hydration leads to the formation of ettringite (Eq. (3)) (Pelletier *et al.* 2010, Trauchessec *et al.* 2015).

$$C_4A_3\bar{S} + 2C\bar{S}H_2 + 34H \rightarrow C_6A\bar{S}_3H_{32} + 2AH_3 \quad (1)$$

$$C_4A_3\bar{S} + 18H \rightarrow C_4A\bar{S}H_{12} + 2AH_3 \quad (2)$$

$$C_4A_3\bar{S} + 8C\bar{S}H_2 + 6CH + 74H \rightarrow 3C_6A\bar{S}_3H_{32} \quad (3)$$

where, $C = CaO$, $A = Al_2O_3$, $\bar{S} = SO_3$ and $H = H_2O$.

The reactions above show that the presence of lime can alter the quantities of hydrates formed. In OPC-CSA blended cement, lime source can be directly supplied from OPC and as a by-product of hydration of OPC (in the form of portlandite). Hence, the presence of OPC would substantially influence the hydration of CSA. On the other hand, the presence of CSA could influence the hydration of OPC as well. In the absence of aluminum hydroxide, C_2S and C_3S (alite and belite, major constituents of OPC) hydrate to form calcium silicate hydrates (CSH) and portlandite (CH) (Eq. (4)), but in the presence of aluminum hydroxide (formed during hydration of ye'elimite), alite and belite hydrate to form stratlingite and portlandite (Eq. (5)).

$$2C_3S + 6H \rightarrow C_3S_2H_3 + 3CH \quad (4)$$

$$C_3S + AH_3 + 6H \rightarrow C_2ASH_8 + CH \quad (5)$$

where, $S = SiO_2$.

Janotka and Krajči (1999) found that 85% CSA and 15% OPC improved the setting time to 60 mins and increased the strength of blended cement mortar. Pelletier *et al.* (2010) analyzed the influence of varying OPC, CSA, and calcium sulfate content on the hydration kinetics of blended cement. Calcium sulfate had little impact on hydration when the OPC/CSA ratio was constant. The higher OPC content resulted in lesser early strength but had a significant influence on long-term properties. Trauchessec *et al.* (2015) studied the hydration mechanism and the strength of OPC-CSA blended mortar. Blended cement with a high percentage of CSA (60%) had a strength of 10 MPa, while in presence of added lime had a strength of 30 MPa. The type of OPC used was also found to have an impact on the performance of blended cement. Shrinkage behavior of blended cement was investigated by Sirtoli *et al.* (2020), while porosimetric and shrinkage behavior was studied by Gastaldi *et al.* (2011).

The above works shown in literature on the OPC-CSA blended cement mostly focused on the hydration kinetics under low water to cement ratios in concrete technology. As aforementioned, the use of OPC-CSA blended cement for geotechnical application (e.g., soil improvement that involves much higher water to cement ratios) has not been studied.

2. Materials and sample preparation

A uniformly graded sand classified as "SP' poorly graded sand according to the Unified Soil Classification System (USCS) was used as a host material. The sand had a 'D_{50}' of 0.71 mm and 'D_{10}' of 0.45 mm. Ordinary Portland Cement Type I (OPC) and Calcium Sulfoaluminate (CSA) cement were used as binding admixtures for the current study. Subramanian *et al.* (2019a) found that the optimum dosage of gypsum required for effective use of CSA (sustainable strength gain in sandy soil) was 30%. When lower gypsum content (ratio of gypsum to binder 'cement + gypsum') was used, ettringite was not formed while higher gypsum content resulted in unreacted gypsum. At 30% gypsum content, the added gypsum was fully utilized, and the ettringite formed did not convert to monosulfate. The XRD patterns of the OPC, CSA, and gypsum are shown in Fig. 1.

The cement content (*CC*) is defined as the ratio of the

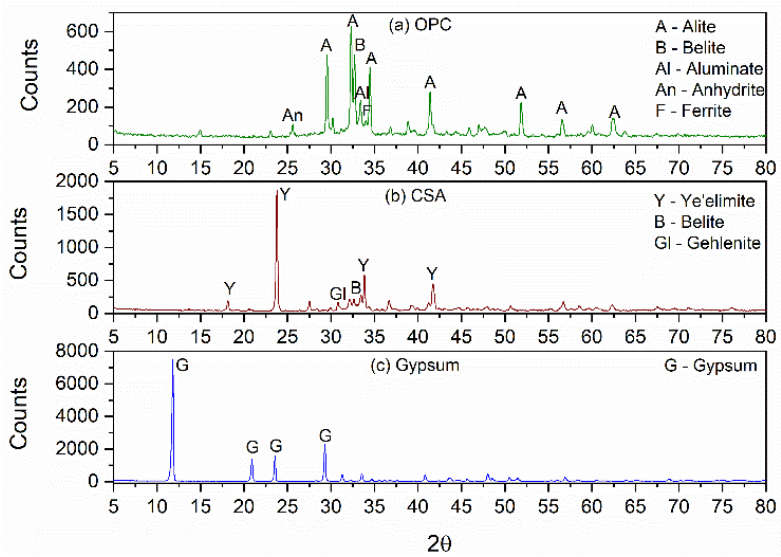

Fig. 1 XRD Pattern of (a) OPC, (b) CSA and (c) Gypsum

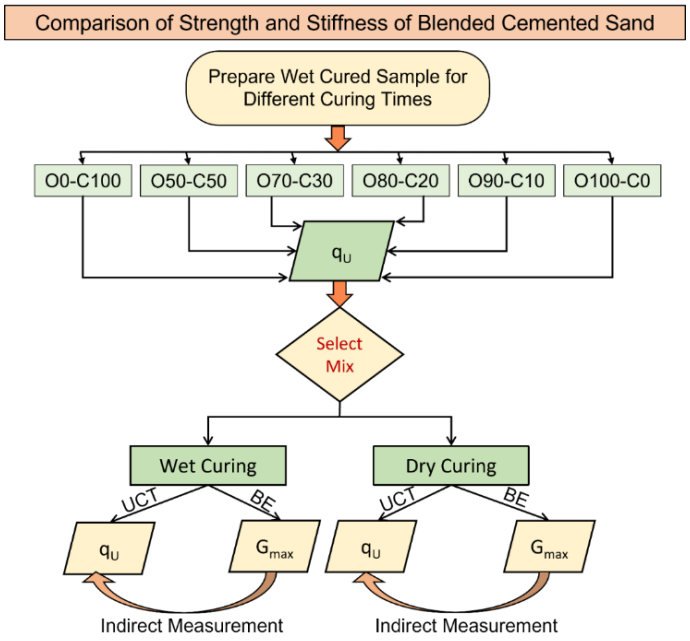

Fig. 2 Experimental plan for the current study

total mass of cement (OPC+CSA) to the mass of dry sand. The water content (w) is defined as the ratio of the mass of water to the mass of solids (cement + sand). In this study, CSA cement refers to 70% CSA and 30% gypsum. The required mass of sand, water, and cement is taken. Firstly, the dry sand and some water are mixed in a Hobart mixer for 5 minutes. Then, the required amount of cement and remaining water are mixed in the Hobart mixer for 5 minutes, after which the remaining water is added and mixed for another 5 minutes. PVC molds of 50mm internal diameter and 100 mm in height are used to prepare samples. The inside of the molds is greased for easy extraction after desired curing time.

The homogenous cemented sand mixture prepared is transferred to the PVC in three layers, and each layer is compacted. Undercompaction technique developed by Ladd (1978) is used, where the bottom layers are compacted less and the top layers are compacted more. This technique enables the samples to be compacted uniformly, as the compaction effort of the top layers is transferred to the bottom layers. The top and bottom of the PVC molds are covered with plastic and kept in water for desired curing period for 'Wet curing' or kept in an empty box for 'Dry curing'. For each mix considered in this study, six samples were prepared, of which five samples were used for strength and stiffness testing while one sample was used to find the moisture content after desired curing time. This moisture content after the desired curing time is referred to as post-

Table 1 Mix design summary to find optimum OPC-CSA blend

Test Name*	Sand (g)	OPC (g)	CSA binder		Cement (OPC+CSA) (g)	Water (g)
			CSA (g)	Gypsum (g)		
O100-C0	1000	70	0	0	70	107
O90-C10		63	4.9	2.1		
O80-C20		56	9.8	4.2		
O70-C30		49	14.7	6.3		
O50-C50		35	24.5	10.5		
O0-C100		0	49	21		

*Test name: 'O' and 'C' indicate OPC and CSA respectively while the number is the percentage of each cement in the blended mixture

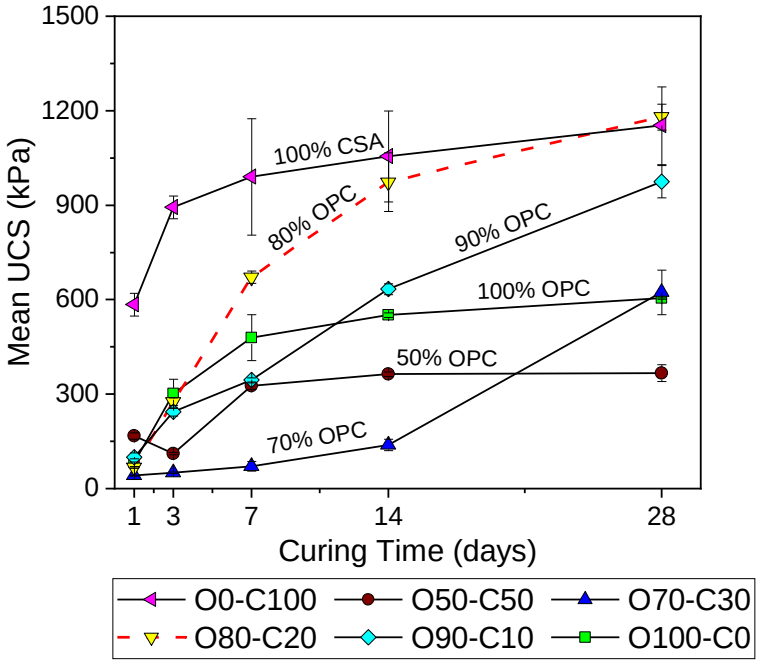

Fig. 3 Unconfined compressive strength development of various OPC-CSA blends at *CC*= 7% and *w*=10%. Note: 'O' and 'C' indicate OPC and CSA respectively while the number is the percentage of each cement in the blended mixture

curing moisture content. The strength and stiffness results are from the best three samples which have smaller standard deviations. After the desired curing time, the samples are removed, and the bulk density is calculated and checked for consistency with ±1% variation between samples. Fig. 2 shows the experimental plan for the current study.

3. Results and discussion

3.1 Optimum OPC-CSA Blend

It is well established in literature that the initial and the ultimate strength gain of CSA treated sand is higher than that of OPC treated sand (Vinoth *et al.* 2018, Subramanian *et al*. 2019a). Since the cost of CSA is much higher than that of OPC, generally it is not economically viable to use CSA treated sand for ground improvement projects. Hence, an optimum blend of OPC-CSA mixture needs to be found such that the cost of ground improvement would be reduced when compared to using CSA only, without compromising the strength of the cemented treated sand. Therefore, four mixtures of OPC-CSA blend along with pure CSA (70% CSA +30% gypsum) and pure OPC treated sand are prepared and tested for unconfined compressive strength to check the effectiveness of the cementation process.

The cement content for this scope of work is kept constant at 7%, and the water content is kept constant at 10%. Both cement and water content being within typical ranges for cement treated sand (Consoli *et al*. 2010, Wei and Ku 2020). The workability is good with the chosen water content and cement content. With the 7% cement content, the proportion of OPC and CSA is varied to create the blended cement. The samples were wet cured, and the curing time adopted was 1, 3, 7, 14, and 28 days, for the optimization study. Only wet curing was chosen for the optimization study because wet cured samples have lower strength than dry cured samples and have more exposure to water (Subramanian *et al.* 2018). The wet curing condition is also expected to better reflect the actual construction sites

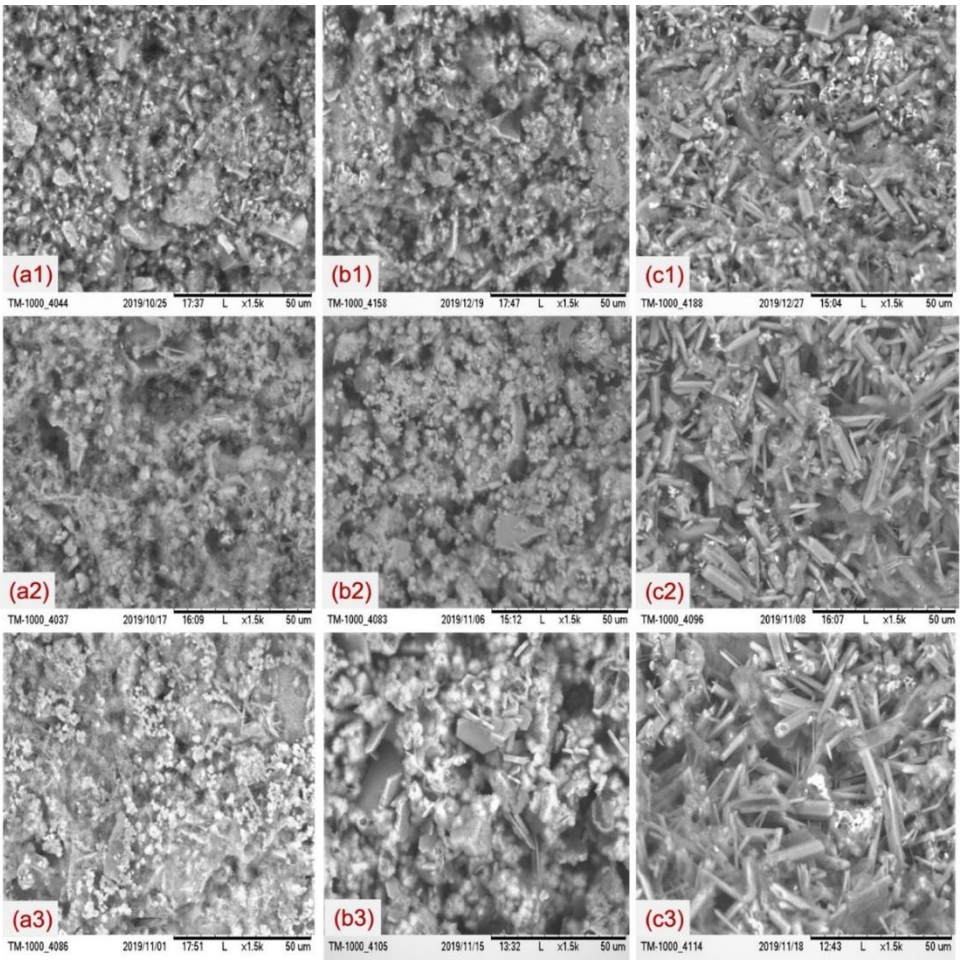

Fig. 4 SEM images of O80-C20 (a1, a2, a3), O100-C0 (b1, b2, b3) and O0-C100 (c1,c2,c3) at 1 day, 7 days and 28 days of curing. Note: 'a', 'b' and 'c' series corresponds to O80-C20, O100-C0 and O0-C100, respectively. The preceding numbers 1, 2 and 3 correspond to 1day, 7 days and 28 days of curing time

in Singapore where the groundwater table is close to the surface. Table 1 shows the mix design opted in this study to find the optimum OPC-CSA blend. Fig. 3 shows the variation of the unconfined compressive strength against curing time.

The pure CSA treated sand has an initial strength (1 day) equivalent to 50% of its ultimate strength (28 days). This high initial strength, as discussed earlier, is due to the hydration of ye'elimite in presence of gypsum to form ettringite. On the other hand, OPC treated sand has an initial strength (1 day) equivalent to 14% of its ultimate strength (28 days). The presence of gypsum in OPC clinker inhibits the early hydration of the aluminate phase of OPC causing the lower initial strength. This trend of low initial strength is observed for OPC dominated mixes. The optimum mix of OPC-CSA based on the unconfined compressive strength seems to be O80-C20, which has a lower initial strength (similar to 100% OPC) but has a gradually increasing trend with an ultimate strength equivalent to that of the pure CSA treated sand, which is significantly higher than the 100% OPC treated sand.

Although only 20% of OPC is replaced with CSA, it would still be eco-friendly than using 100% OPC, considering that the ground improvement or land reclamation work involves cement stabilization of several million m^3 of soil. The optimum blended cement ratio exhibits the early gain characteristics of OPC and the ultimate strength characteristics of CSA. Hence, this blended cement would be ideal for the case where rapid hardening is not required but sustainable and controlled strength increase is desirable.

3.2 Microstructure from SEM

Fig. 4 shows the SEM images of O80-C20, O100-C0, and O0-C100 at the end of 1, 7, and 28 days of curing. Fig. 6 shows the SEM images of O90-C10, O70-C30, and O50-C50 at the end of 1, 7 and 28 days. 'O' and 'C' indicate OPC and CSA respectively while the number is the percentage of each cement in the blended mixture.

3.2.1 Observations after of 1 day curing

1 day hydration of ye'elimite (present in O0-C100 blend) is found to be enriched with ettringite Fig. 4(c1)) resulting in higher initial strength. But, 1 day hydrated O80-C20 blend shows the loose formation of CSH (fibrous and irregular) along with the weak formation of ettringite (Fig. 4 (a1)) resulting in lower initial strength. On the other hand,

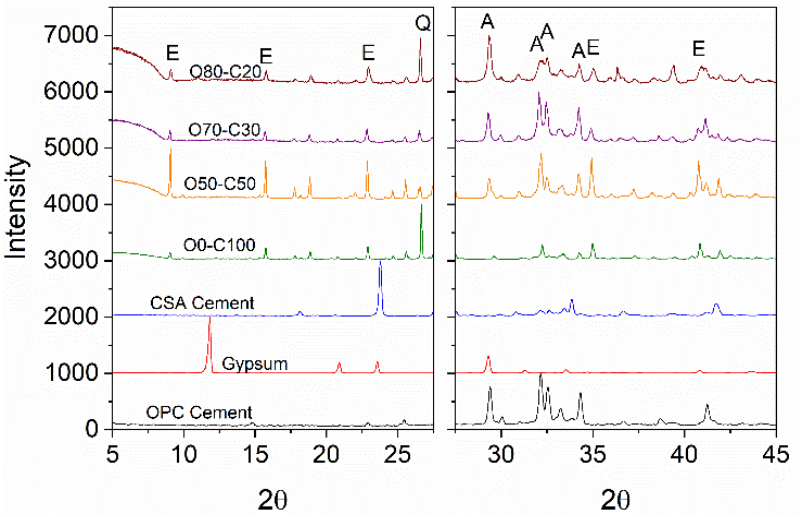

Fig. 5 XRD Analysis of 1 day cured cemented sand with different blends of OPC and CSA. (Note: E = Ettringite, A= Alite, Q=Quartz)

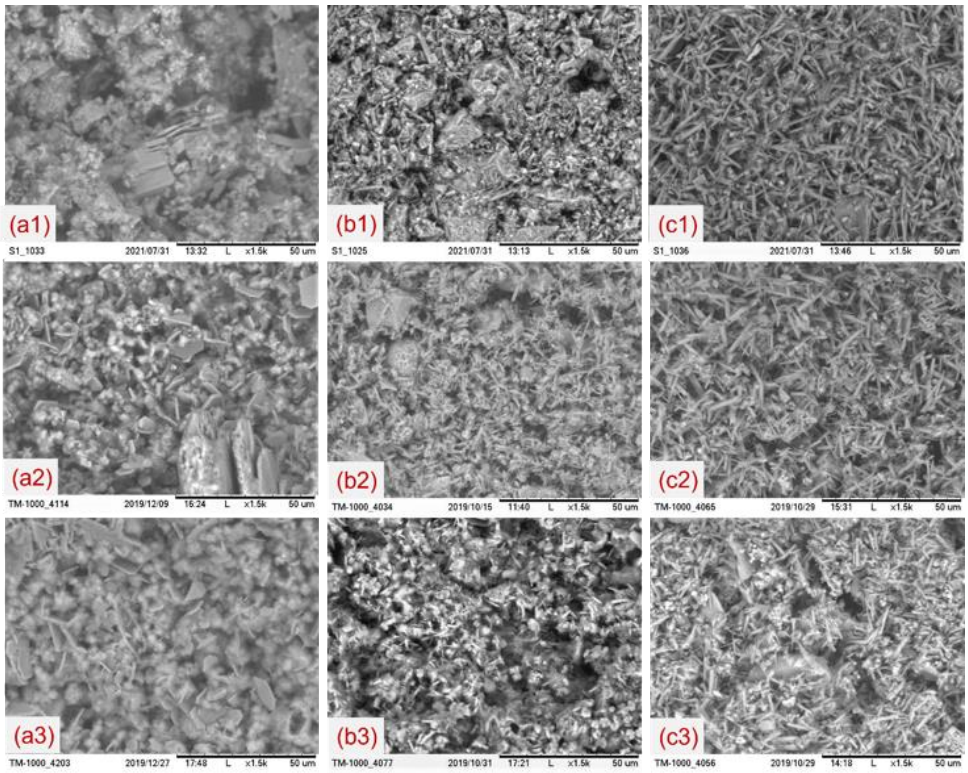

Fig. 6 SEM images of O90-C10 (a1,a2,a3), O70-C30 (b1,b2,b3) and O50-C50 (c1,c2,c3) at 1 day, 7 days and 28 days of curing. Note: 'a', 'b', and 'c' series correspond to O90-C10, O70-C30 and O50-C50, respectively. The preceding numbers 1, 2 and 3 correspond to 1 day, 7 days and 28 days of curing time

the structure of 1 day cured O80-C20 looks similar to the 1-day hydration of O100-C0 (Fig. 4(b1)), where only the presence of fibrous CSH can be seen. The SEM observations are complemented by the XRD analysis shown in Fig. 5.

In XRD, after 1 day of curing, O80-C20 shows the presence of ettringite and unreacted alite (which cannot be seen in the SEM used in this study). The absence of rich formation of ettringite and the presence of loose formation of CSH along with unreacted alite explains the low initial strength of O80-C20 blend treated sand. SEM image of 1-day hydrated O90-C10 blend shows the loose formation of CSH from hydration of alite and hexagonally shaped calcium hydroxide, a by-product of alite reacting with water (Fig. 6(a1)). Hydration of O70-C30 shows loose formation of ettringite (Fig. 6(a2)), while, hydration of O50-C50 shows rich formation of ettringite (Fig. 6(a3)), which is complemented by XRD analysis (Fig. 5).

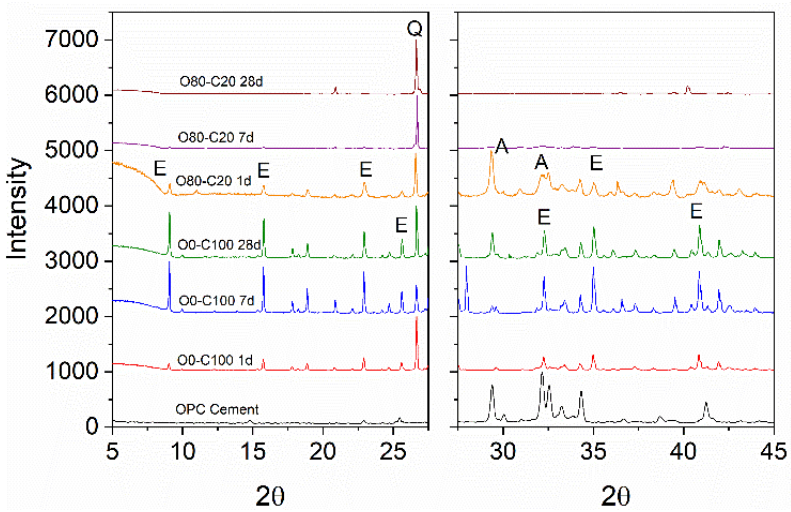

Fig. 7 XRD analysis of 1 day, 7 days, and 28 days cured samples of O80C20 and O0C100

3.2.2 Observations after 7 days of curing

In case of OPC treated sand, alite continues to hydrate to form calcium silicate hydrate which can be seen in SEM images as shown in Fig. 4(b2), while, the ye'elimite present in the CSA treated sand continues to hydrate in presence of gypsum to form ettringite as shown in Fig. 4(c2). SEM image of hydrated O90-C10 blend (Fig. 6(a2)) shows the formation of CSH along with hexagonally shaped calcium hydroxide (OPC dominated system), while hydration of O80-C20 blend shows a loose formation of CSH followed by a trace of ettringite (Fig. 4(a2)). These observations are consistent with the XRD results shown in Fig. 7. SEM image of 7 days hydrated O70-C30 blend shows the significant formation of ettringite (Fig. 6 (b2)). On the other hand, hydration of O50-C50 blend results in porous ettringite formation for 7 days curing (Fig. 4 (c2)).

3.2.3 Observations after 28 days of curing

At the end of 28 days of curing, O100-C0 treated sand shows the formation of fibrous CSH structure and hexagonally shaped calcium hydroxide (Fig. 4(b3)), which indicates no pozzolanic reaction as expected, while O0-C100 treated sand shows a dense and rich formation of ettringite (Fig. 4(c3)). Hydration of O90-C10 shows the presence of calcium hydroxide and fibrous CSH structure (Fig. 6 (a3)), similar to that of O100-C0 (Fig. 4(b3)) after 28 days of curing. On the other hand, 28 day hydrated O80-C20 blend (Fig. 4(a3)) shows a dense structure with the presence of CSH and the absence of calcium hydroxide, while the XRD analysis of O80C20 blend (Fig. 7) shows no traces of unreacted alite which was present after 1 day of curing. 28-day SEM image of hydrated O70-C30 blend shows significant CSH formation and minor traces of ettringite Fig. 6(b3)), while O50-C50 blend results in porous ettringite formation after 28 days hydration (Fig. 6 (c3)). This study focuses more on the mechanical behavior of the OPC-CSA blend, while the microstructure observations are presented for completion of the section. These observations made from the SEM images and the XRD analysis of the hydrated products may provide some insights to better understand the association of these microstructural evolutions to the strength variations observed, but these are not in the main scope of this study.

The complex strength development of "ternary" system of OPC, CSA, and gypsum which cannot be clearly explained considering its intrinsic complex hydration of each component as well as their interaction. Based on the SEM and XRD knowledge combined with the strength testing, the following hypothesis is proposed.

The six samples are divided into three groups for the interpretation. There is a clear acceleration and strength enhancement as follows: O100-C0 < O90-C10 < O80-C20. This can be explained by the well-known reaction between OPC and gypsum (rather than the addition of CSA). The gypsum can facilitate sulfate reaction and promote the formation of thermo-dynamically stable ettringite crystal. It can contribute to the acceleration and strength development. Especially, the ettringite formation reaction is expansive so that the effect of the formation on the strength development can be more significant in cemented sand system (i.e., much more porous than regular cement-based composites). Therefore, we believe the enhancement of early material performance in O100-C0, O90-C10 and O80-C20 can be more affected by the increased amount of gypsum rather than CSA.

Then there is a sudden drop of strength from O80-C20 to O70-C30. It is an interesting observation that the strength development of O70-C30 is slower till 14 days. False setting can be the main reason of this phenomenon. The false setting is due to the too much amount of gypsum in OPC which should be avoided practically. In this case, gypsum crystallization occurs rather than sulfate supply for OPC hydration. We think even in this case, gypsum is playing more pivoting role than CSA.

Then, it is observed that the enhancement of material performance has the following trend: O70-C30 < O50-C50 < O0-C100. This can be due to the intended reaction of CSA. In the CSA, there is ye'elimite crystal which reacts with sulfate to form ettringite crystal. As mentioned previously, the ettringite formation is fast and stable at very

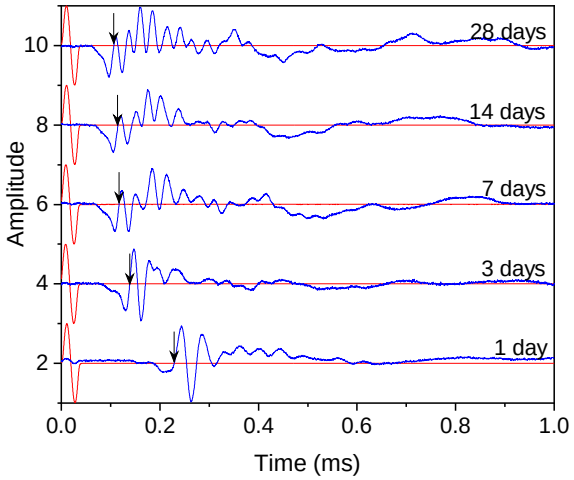

Fig. 8 Signals generated from bender element (BE) testing with 30kHz input frequency. The sample tested was wet cured with *CC*=5%, *w*=10%

early age. Hence, the effect of CSA-induced ettringite formation can be prominent in O50-C50 and O0-C100 as they showed much sudden increase of initial strength development.

As initially stated, the intended system has many experimental variables which can lead to the intrinsic complex hydration behaviors in cement-related materials. Several phases exist in OPC and CSA each, and they react with water along and interact each other. The system investigated herein is very special application for cemented sand which is much more porous than normal application of OPC or CSA. Therefore, more scientific research needs to be conducted to elucidate the complex reactions in the future.

3.3 Parametric study

An OPC-CSA mix with 80% OPC and 20% CSA was found to be the optimum blend as the ultimate strength (28 days) was equivalent to that of CSA cemented sand with a gradually increasing trend. Based on the identified optimum blend, a detailed parametric study is conducted to investigate the behavior of blended cement treated sand when the cement and moisture contents are varied.

3.3.1 Bender element testing

Apart from measuring unconfined compressive strength, bender element (BE) testing is also conducted to characterize the small strain shear stiffness of blended cement treated sand under geotechnical environment (i.e., higher water to cement ratio than concrete technology). Bender elements consist of a piezoceramic material, which converts voltage to mechanical disturbance and vice versa. Because of the piezoceramic transducers, the bender elements can generate and receive shear waves. Using the bender element signals, the shear wave velocity is calculated based on the travel distance, which is the tip-to-tip distance (L_{tt}) between the bender elements, and the time required to cover the travel distance. Small strain shear stiffness is then calculated from the shear wave velocity (V_S) using $G_{max} = \rho \times V_S^2$. Herein, ρ is the bulk density of cemented soil. Disturbance caused by the bender element for generating shear wave is within the elastic threshold, making it more suitable for small strain studies.

The bender element used in this study had a width of 12 mm, a thickness of 3mm, and a cantilever length of 2.5 mm. To ensure a tight coupling between the bender and the cemented sand, a groove of 2.5 mm is made on both ends of the cemented sample, and plasticine is placed in the groove to ensure good contact. The presence of plasticine as a filler in the groove does not affect the shear wave velocity of the cemented soil (Xiao *et al.* 2018). A signal generator (Keysight technologies 33210A) is used to generate a sinusoidal pulse with an input voltage of 20V and an input frequency of 30 kHz. The sampling frequency is set at 4 MHz or 20000 samples in 5ms. This input frequency covers the stabilizing part of the wave path to wavelength (L/λ) ratio (Moon *et al.* 2020, Subramanian *et al.* 2020a). The zero crossing after the first bump of the received signal (marked with arrows in Fig. 8) is taken as the arrival time of the shear wave, which is subsequently used in calculating shear wave velocity. Fig. 8 shows the input and output signals from a bender element testing on wet cured samples with *CC*=5%, *w*=10% at various curing times.

3.3.2 Small strain shear modulus and unconfined compressive strength

Once the shear wave velocity is obtained, the small strain shear modulus of the cemented sample is calculated based on the bulk density of sample. Fig. 9 shows the variation of small strain shear modulus with curing time for cement treated sand under wet and dry curing conditions. The small strain shear modulus of the cement treated soil increases with curing time for both wet and dry curing conditions.

The unconfined compressive strength, shown in Fig. 10, also follows the same trend as the small strain shear modulus. As the curing time increases, more cement is

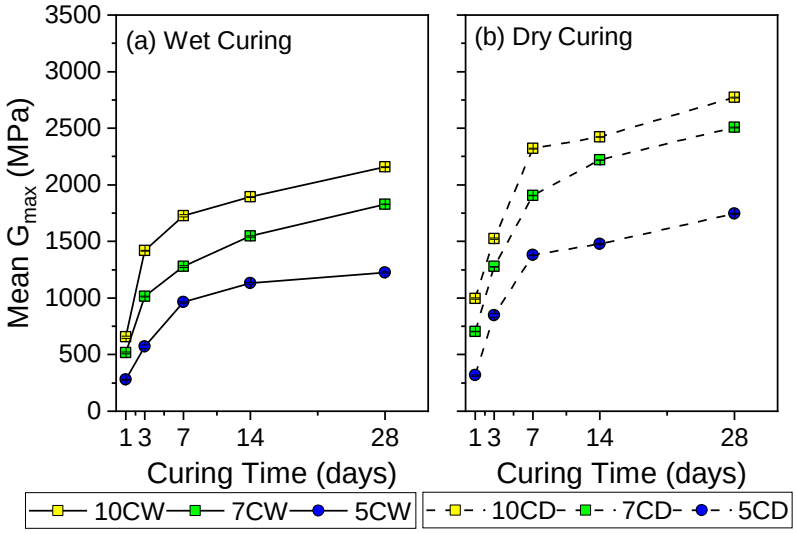

Fig. 9 Variation of small strain shear modulus with curing time for (a) wet cured and (b) dry cured samples. (Note: 10CW – Numerals indicate the cement content in %, C stands for cement and W stands for wet curing. 7CD means 7% cement content and dry curing)

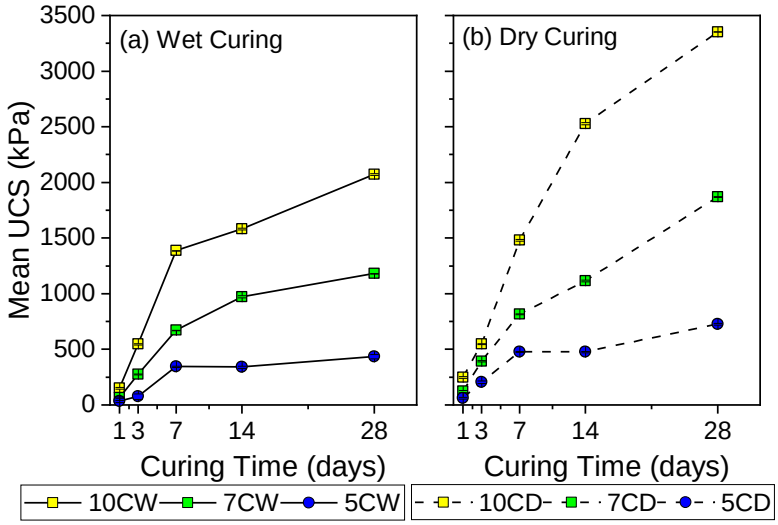

Fig. 10 Variation of unconfined compressive strength with curing time for (a) wet cured and (b) dry cured samples

exposed to water, thereby resulting in more cementitious hydration products formed with curing time, which helps in increasing the stiffness and strength of cemented sand.

Also, irrespective of the cement content, the initial water content is kept constant at 10%, thereby reducing the initial water to cement ratio as the cement content increases. A reduction in the water to cement ratio would lead to a less porous hydrated cement structure, which would further contribute to the increasing strength and stiffness with an increase in cement content. Fig. 11 shows the variation of unconfined compressive strength against the initial water to cement ratio for both dry and wet curing conditions. The strength reduces with increasing the initial water to cement ratio. A similar trend was observed by Wei *et al.* (2020).

As a useful design parameter, the concept of adopting the porosity to volumetric cement content ratio (η/C_{iv}) was proposed by Consoli *et al.* (2007) to characterize the strength of cemented sands. η/C_{iv} is the volumetric expression of the water to cement ratio, which is calculated based on the volume of water and cement. The porosity (η) is calculated from void ratio (e), $\eta = e/(1+e)$. The void ratio is then calculated from bulk density as follows, $\rho_b = \frac{G\rho_w}{1+e}(1+w)$, where '$G$' is the specific gravity of cemented soil, 'ρ_b' is the bulk density of cemented soil, 'e' is the void ratio and 'w' is the water content. The volumetric cement content is calculated from phase diagram as the cement and water content used is known in terms of mass. Through phase diagram, these quantities are converted to their respective volumetric proportions and the volumetric cement content is calculated. Fig. 12 shows the variation of unconfined compressive strength with η/C_{iv}.

Both the wet cured and dry cured samples are prepared with the same procedure, except that the wet cured sample is cured under water while the dry cured samples are not exposed to water. Although the range of η/C_{iv} is the same,

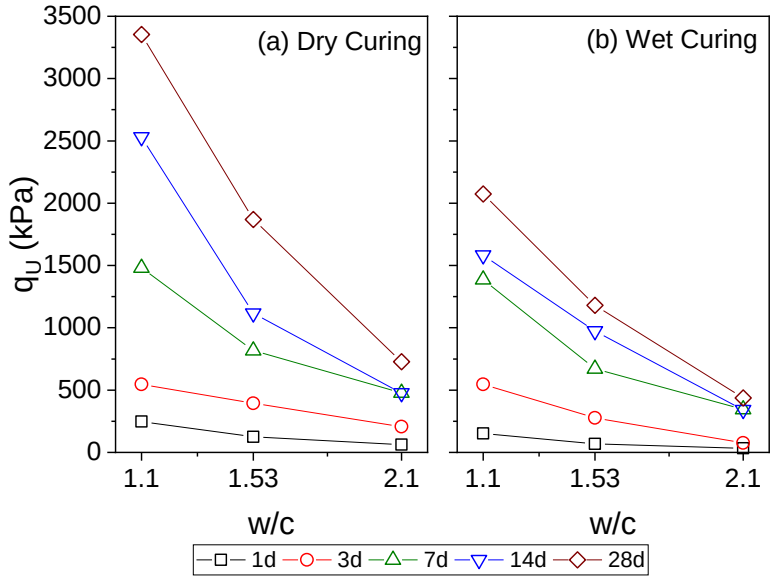

Fig. 11 Variation of unconfined compressive strength with water to cement ratio (a) Dry Curing and (b) Wet Curing

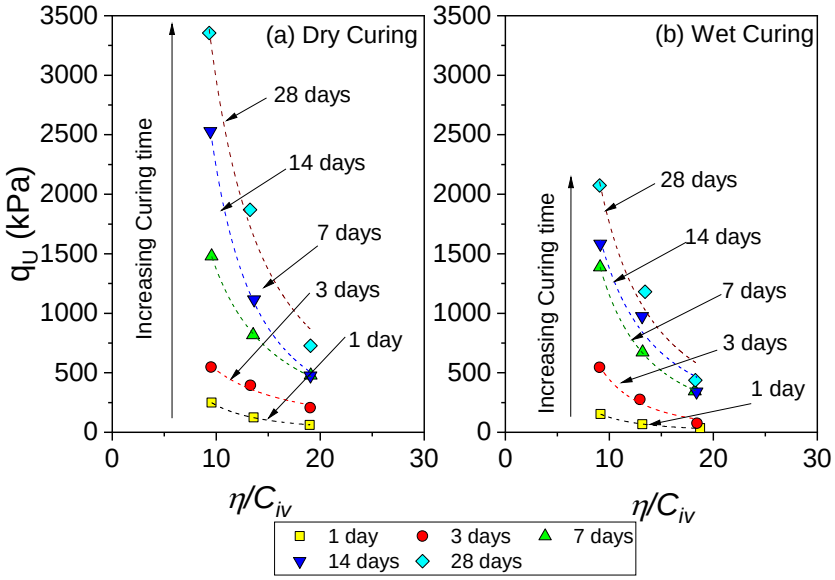

Fig. 12 Variation of unconfined compressive strength with the porosity to volumetric cement content ratio at different curing times for (a) dry cured samples and (b) wet cured samples

the strength of dry cured samples is higher than that of wet cured samples. The difference in the strength of dry and wet cured samples is discussed in the next section.

3.3.3 Comparison between wet and dry curing conditions

Strength and stiffness of cemented samples are higher in dry curing conditions than in wet curing conditions. The testing results show that the strength of the wet cured samples is about 33% lower than the strength of dry cured samples (Fig. 13(a)), and the stiffness of wet cured samples is 25% lower than that of dry cured samples (Fig. 13(b)). It is important to note the manner in which samples were cured to explain the difference between wet and dry curing conditions.

In wet curing conditions, the samples were submerged in water, where the amount of water surrounding the sample is higher than the amount of water inside the sample. Hence, the water in the curing bath enters the samples as indicated by the increase in moisture content from the initial moisture content, as shown in Fig. 14. Irrespective of cement content, just after 1 day of curing, the moisture content has increased from the initial moisture content of 10% to the post-curing moisture content of 15%.

In dry curing conditions, the samples are kept in an empty curing bath. Hence, the cemented sand hydrates under the moisture content available within the sand, thereby reducing the post-curing moisture content of the sample, as shown in Fig. 14. Also, it is important to note that the water inside the sample did not escape due to the

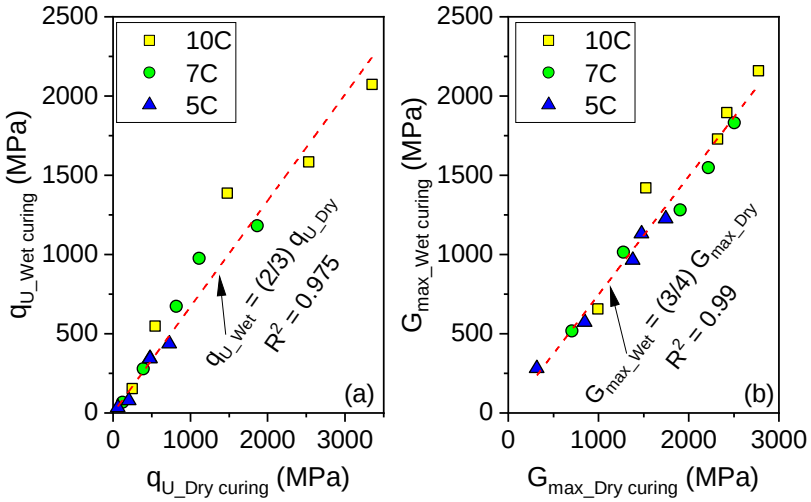

Fig. 13 Comparison between wet curing and dry curing on (a) unconfined compressive strength and (b) small strain shear modulus

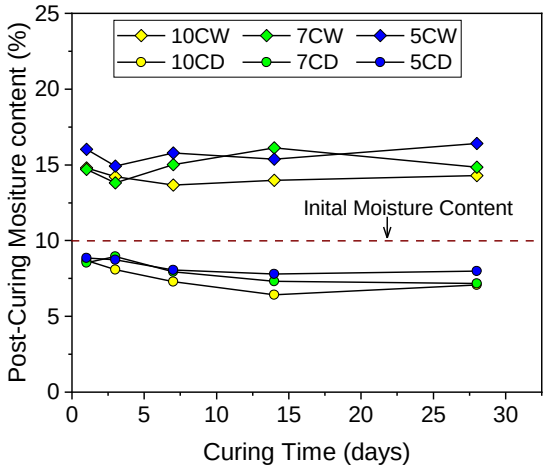

Fig. 14 Variation of initial moisture content with curing time for both wet and dry curing conditions

dry curing conditions outside the sample, because no excess water was seen on the curing bath, thereby indicating the water was used for hydration reaction. It is well established that the hydrated cement structure is porous & weak at higher moisture content and strong & less porous at lower moisture content, thereby affecting the strength and stiffness of cemented sand under wet and dry curing conditions (Claisse 2016).

The deviation of post-curing moisture content from initial moisture content for both wet cured and dry cured samples does not affect the initial porosity of the cemented sand. The compacted cemented sand has an initial pore arrangement before it is kept for curing (either dry or moist curing). The excess water (water other than the initial moisture) intruding the sample in case of wet curing occupies the existing voids of the cemented sand, without causing significant change to initial porosity. It should be noted that the excess water would make the cement paste porous without altering the structure of entire cemented sand. Similarly, the water available in the cemented sand matrix is consumed during hydration under dry curing condition, without causing significant changes to the existing pore structure. Hence the analysis shown in Fig. 12 is still valid.

Subramanian *et al.* (2018) hypothesized that the wet cured samples were fully saturated due to the water seeping into the sample from the curing bath while the dry cured samples were partially saturated as the cement hydration consumes the water in the cemented sand, hence this difference in the degree of saturation could be one of the contributing mechanisms to the increased strength and stiffness of cemented sand under dry curing conditions. For instance, the higher strength and stiffness observed in dry curing would be explained by matric suction generated inside the dry samples. Mindess *et al.* (2002) reported that the presence of excess water would alter the characteristics of the hydration product. For example, in the case of OPC, the presence of excess water would weaken the van der Waals forces in the primary hydration product, calcium silicate hydrate, thereby reducing the strength of OPC

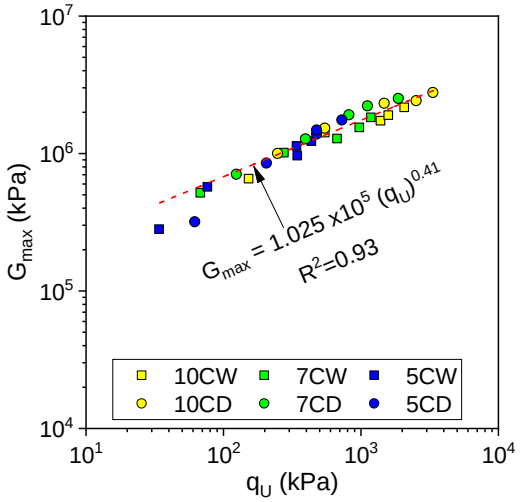

Fig. 15 Relationship between small strain shear modulus and unconfined compressive strength.

treated sand. Similar to these observations, the OPC dominated blended cement (O80C20) in this study also showed an identical trend between dry and wet curing.

3.3.4 q_U - G_{max} relationship

Small strain shear modulus testing through wave-based techniques is non-destructive in nature (measurements within elastic ranges), whereas strength testing is destructive since a failure mechanism is involved. Hence, an empirical relationship between these two parameters would help in predicting the strength of the cemented soils through non-destructive testing methods, at least as a first-order estimation. This relationship would be more useful for practicing engineers in determining the QA/QC of the cement treated soil. Fig. 15 shows the power relationship between the strength and stiffness of blended cement treated sand with a coefficient of determination (R^2) of 0.93. Since it is an empirical relationship, it would apply only to the ranges of strength (50 kPa to 3500 kPa) and stiffness (250 MPa to 2750 MPa) tested in this study.

4. Conclusions

The objective of the study was to partly replace OPC with CSA cement, thereby enhancing the mechanical behavior of OPC cement and also reducing the carbon footprint. 100% CSA cement treated sand would have great material performance but not economically applicable for large projects. Therefore, the partial replacement of OPC to achieve similar mechanical properties as CSA treated sand can be beneficial. Some important findings in this study are summarized.

- An OPC-CSA blend with 80% OPC and 20% CSA yielded unconfined compressive strength similar to that of 100% CSA treated sand. Although the initial strength of the blended cement was much lower than that of 100% CSA treated sand, the ultimate strength achieved by blended cement was comparable to that of CSA treated sand.
- The microstructural analysis of O80-C20 indicated that ye'elimite present in CSA hydrated within 1 day, while unreacted alite was present in the XRD analysis after 1 day curing. A dense CSH structure was formed at the end of 28 days curing.
- Parametric studies indicated that the strength and stiffness gain with curing time was hyperbolic for both wet and dry cured samples, which is good for targeting sustainable and controlled strength development of cemented soil. The strength of wet cured samples was 33% lower than the dry cured samples, while the stiffness of the wet cured samples was 25% lower than the dry cured samples. These findings will be useful in taking into account the effect of groundwater when designing cement treated ground improvements.
- In dry curing condition, the samples are cured under the existing moisture content, thereby resulting in lower post-cured moisture content. In the case of wet curing, excess water was available from the curing bath, thereby increasing the post-curing moisture content of the samples. This is one of the main reasons for the strength and/or stiffness difference observed between dry and wet cured samples.
- There exists an empirical relationship between stiffness and strength. Hence, non-destructive wave-based measurement could be useful for QA/QC determination for practicing engineers.

Acknowledgments

The authors appreciate the financial support from the Singapore Ministry of Education (PI –Ku, Taeseo; Award Number: R-302-000-194-114) and Konkuk University.

References

Chaunsali, P. and Mondal, P. (2015), "Influence of calcium sulfoaluminate (CSA) cement content on expansion and hydration behavior of various ordinary portland cement-CSA

blends", *J. Am. Ceramic Soc*., **98**(8), 2617-2624. https://doi.org/10.1111/jace.13645.

Choi, S.G., Chu, J. and Kwon, T.H. (2019), "Effect of chemical concentrations on strength and crystal size of biocemented sand", *Geomech. Eng*., **17**(5), 465-473. https://doi.org/10.12989/gae.2019.17.5.465.

Claisse, P.A. (2016), Chapter 20 - Hydration of cement. *Edited by* P.A.B.T.-C.E.M. Claisse. Butterworth-Heinemann, Boston, 189-200.

Consoli, N.C., Cruz, R.C., Floss, M.F., Festugato, L., Consoli, C.N., Caberlon, C.R., Felipe, F.M. and Lucas, F. (2010), "Parameters controlling tensile and compressive strength of artificially cemented sand", *J. Geotech. Geoenviron. Eng*., **136**(5), 759-763.

Consoli, N.C., Foppa, D., Festugato, L. and Heineck, K.S. (2007), "Key parameters for strength control of artificially cemented soils", *J. Geotech. Geoenviron. Eng*., **133**(2), 197-205. https://doi.org/10.1680/geot.8.P.084.

Consoli, N.C., Párraga Morales, D. and Saldanha, R.B. (2021), "A new approach for stabilization of lateritic soil with Portland cement and sand: Strength and durability", *Acta Geotechnica*, **16**(5), 1473-1486. https://doi.org/10.1007/s11440-020-01136-y.

Consoli, N.C.C., Fonseca, A.V. d. V. da, Silva, S.R.R., Cruz, R.C.C. and Fonini, A. (2012), "Parameters controlling stiffness and strength of artificially cemented soils", *Geotechnique*, **62**(2), 177-183. https://doi.org/10.1680/geot.8.p.084.

Gastaldi, D., Canonico, F., Capelli, L., Bianchi, M., Pace, M., Telesca, A. and Valenti, G. (2011), "Hydraulic behaviour of calcium sulfoaluminate cement alone and in mixture with portland cement", *Proceedings of the* 13th *International Congress on the Chemistry of Cement*, Madrid, Spain, July.

Horpibulsuk, S., Bergado, D.T. and Lorenzo, G.A. (2004), "Compressibility of cement-admixed clays at high water content", *Geotechnique*, **54**(2), 151-154. https://doi.org/10.1680/geot.2004.54.2.151.

Huang, G., Pudasainee, D., Gupta, R. and Liu, W.V. (2021), "Extending blending proportions of ordinary Portland cement and calcium sulfoaluminate cement blends: Its effects on setting, workability, and strength development", *Front. Struct. Civil Eng*., **15**(5), 1249-1260. https://doi.org/10.1007/s11709-021-0770-4.

Janotka, I. and Krajči, U. (1999), "An experimental study on the upgrade of sulfoaluminate-belite cement systems by blending with Portland cement", *Adv. Cement Res*., **11**(1), 35-41. https://doi.org/10.1680/adcr.1999.11.1.35.

Juenger, M.C.G., Winnefeld, F., Provis, J.L. and Ideker, J.H. (2011), "Advances in alternative cementitious binders", *Cement Concrete Res*., **41**(12), 1232-1243. https://doi.org/10.1016/j.cemconres.2010.11.012.

Jumassultan, A., Sagidullina, N., Kim, J., Ku, T. and Moon, S.W. (2021), "Performance of cement-stabilized sand subjected to freeze-thaw cycles", *Geomech. Eng*., **25**(1), 41-48. https://doi.org/10.12989/gae.2021.25.1.041.

Khan, Q., Subramanian, S., Wong, D.Y.C.D.Y.C. and Ku, T. (2019), "Bender elements in stiff cemented clay: shear wave velocity correction by applying wavelength considerations", *Can. Geotech. J*., **56**(7), 1034-1041. https://doi.org/10.1139/cgj-2018-0153.

Ladd, R.S. (1978), "Preparing test specimens using undercompaction", *Geotech. Test. J*., **1**(1), 16-23. https://doi.org/10.1520/GTJ10364J.

Lan, W. and Glasser, F.P. (1996), "Hydration of calcium sulphoaluminate cements", *Adv. Cement Res*., **8**(31), 127-134. https://doi.org/10.1680/adcr.1996.8.31.127.

Lee, C., Nam, H., Lee, W., Choo, H. and Ku, T. (2019), "Estimating UCS of cement-grouted sand using characteristics of sand and UCS of pure grout", *Geomech. Eng*., **19**(4), 343-352. https://doi.org/10.12989/gae.2019.19.4.343.

Mehdipour, I. and Khayat, K.H. (2018), "Effect of shrinkage reducing admixture on early expansion and strength evolution of calcium sulfoaluminate blended cement", *Cement Concrete Compos*., **92**, 82-91. https://doi.org/10.1016/j.cemconcomp.2018.06.002.

Mindess, S., Young, J.F. and Darwin, D. (2002), Concrete. 2nd Ed., Prentice Hall, Upper Saddle River, N.J.

Moon, S.W.W., Vinoth, G., Subramanian, S., Kim, J. and Ku, T. (2020), "Effect of fine particles on strength and stiffness of cement treated sand", *Granular Matter*, **22**(1), 1-13. https://doi.org/10.1007/s10035-019-0975-6.

Park, S., Jeong, Y., Moon, J. and Lee, N. (2021), "Hydration characteristics of calcium sulfoaluminate (CSA) cement/portland cement blended pastes", *J. Build. Eng*., **34**, 101880.

Pelletier, L., Winnefeld, F. and Lothenbach, B. (2010), "The ternary system Portland cement-calcium sulphoaluminate clinker-anhydrite: Hydration mechanism and mortar properties", *Cement Concrete Compos*., **32**(7), 497–507. https://doi.org/10.1016/j.cemconcomp.2010.03.010.

Pooni, J., Robert, D., Giustozzi, F., Setunge, S., Xie, Y.M. and Xia, J. (2021), "Performance evaluation of calcium sulfoaluminate as an alternative stabilizer for treatment of weaker subgrades", *Transportation Geotech.*, **27**, 100462. https://doi.org/10.1016/j.trgeo.2020.100462.

Rios, S., Viana da Fonseca, A. and Baudet, B.A. (2014), "On the shearing behaviour of an artificially cemented soil", *Acta Geotechnica*, **9**(2), 215-226. https://doi.org/10.1007/s11440-013-0242-7.

Saberian, M., Moradi, M., Vali, R. and Li, J. (2018), "Stabilized marine and desert sands with deep mixing of cement and sodium bentonite", *Geomech. Eng*., **14**(6), 553-562. https://doi.org/10.12989/gae.2018.14.6.553.

Sagidullina, N., Abdialim, S., Kim, J., Satyanaga, A. and Moon, S.W. (2022), "Influence of freeze–thaw cycles on physical and mechanical properties of cement-treated silty sand", *Sustainability*, **14**(12), 7000. https://doi.org/10.3390/su14127000.

Shen, Z., Gao, F., Wang, Z. and Jiang, M. (2019), "Evolution of mesoscale bonded particle clusters in cemented granular material", *Acta Geotechnica*, **14**(6), 1653-1667. https://doi.org/10.1007/s11440-019-00850-6.

Shooshpasha, I. and Shirvani, R.A. (2015), "Effect of cement stabilization on geotechnical properties of sandy soils", *Geomech. Eng*., **8**(1), 17-31. https://doi.org/10.12989/gae.2015.8.1.017.

Sirtoli, D., Wyrzykowski, M., Riva, P. and Lura, P. (2020), "Autogenous and drying shrinkage of mortars based on Portland and calcium sulfoaluminate cements", *Materials and Structures/Materiaux et Constructions*, **53**(5), 1-14. https://doi.org/10.1617/s11527-020-01561-1.

Subramanian, S., Khan, Q. and Ku, T. (2019a), "Strength development and prediction of calcium sulfoaluminate treated sand with optimized gypsum for replacing OPC in ground improvement", *Constr. Build. Mater.*, **202**, 308-318. https://doi.org/10.1016/j.conbuildmat.2018.12.121.

Subramanian, S., Khan, Q. and Ku, T. (2020a), "Effect of sand on the stiffness characteristics of cement-stabilized clay", *Constr. Build. Mater*., **264**, 120192. https://doi.org/10.1016/j.conbuildmat.2020.120192.

Subramanian, S., Moon, S.W. and Ku, T. (2019b), "Effect of Gypsum on the strength of CSA treated sand", *Proceedings of the 16th Asian Regional Conference on Soil Mechanics and Geotechnical Engineering*.

Subramanian, S., Moon, S.., Moon, J. and Ku, T. (2018), "CSA-treated sand for geotechnical application: Microstructure

analysis and rapid strength development", *J. Mater. Civil Eng*., **30**(12), 04018313. https://doi.org/10.1061/(asce)mt.1943-5533.0002523.

Subramanian, S., Zhang, Y., Vinoth, G., Moon, J. and Ku, T. (2020b), "Hydraulic conductivity of cemented sand from experiments and 3D image based numerical analysis", *Geomech. Eng*., **21**(5), 423-432. https://doi.org/10.12989/gae.2020.21.5.423.

Trauchessec, R., Mechling, J.M., Lecomte, A., Roux, A. and Le Rolland, B. (2014), "Impact of anhydrite proportion in a calcium sulfoaluminate cement and Portland cement blend", *Adv. Cement Res*., **26**(6), 325-333. https://doi.org/10.1680/adcr.13.00051.

Trauchessec, R., Mechling, J.M., Lecomte, A., Roux, A. and Le Rolland, B. (2015), "Hydration of ordinary Portland cement and calcium sulfoaluminate cement blends", *Cement Concrete Compos*., **56**, 106-114. https://doi.org/10.1016/j.cemconcomp.2014.11.005.

Vinoth, G., Moon, S.W., Moon, J. and Ku, T. (2018), "Early strength development in cement-treated sand using low-carbon rapid-hardening cements", *Soils Found*., **58**(5), 1200-1211. https://doi.org/10.1016/j.sandf.2018.07.001.

Wei, X. and Ku, T. (2020), "New design chart for geotechnical ground improvement: characterizing cement-stabilized sand", *Acta Geotechnica*, **15**(4), 999-1011. https://doi.org/10.1007/s11440-019-00838-2.

Wei, X., Liu, H. and Ku, T. (2020), "Microscale analysis to characterize effects of water content on the strength of cement-stabilized sand–clay mixtures", *Acta Geotechnica*, **15**(10), 2905-2923. https://doi.org/10.1007/s11440-020-01018-3.

Winnefeld, F. and Lothenbach, B. (2010), "Hydration of calcium sulfoaluminate cements-experimental findings and thermodynamic modelling", *Cement Concrete Res*., **40**(8): 1239-1247. https://doi.org/10.1016/j.cemconres.2009.08.014.

Winnefeld, F., Martin, L.H.J., Müller, C.J. and Lothenbach, B. (2017), "Using gypsum to control hydration kinetics of CSA cements", *Constr. Build. Mater*., **155**, 154-163. https://doi.org/10.1016/j.conbuildmat.2017.07.217.

Wolf, J.J., Jansen, D., Goetz-Neunhoeffer, F. and Neubauer, J. (2019), "Mechanisms of early ettringite formation in ternary CSA–OPC–anhydrite systems", *Adv. Cement Res*., **31**(4), 195-204.

Xiao, H., Yao, K., Liu, Y., Goh, S.H. and Lee, F.H. (2018), "Bender element measurement of small strain shear modulus of cement-treated marine clay – Effect of test setup and methodology", *Constr. Build. Mater*., **172**, 433-447. https://doi.org/10.1016/j.conbuildmat.2018.03.258.

Yao, K., Xiao, H., Chen, D.H. and Liu, Y. 2018. "A direct assessment for the stiffness development of artificially cemented clay", *Géotechnique*, 1-7. https://doi.org/10.1680/jgeot.18.t.010.

Yilmaz, Y., Cetin, B. and Kahnemouei, V.B. (2017), "Compressive strength characteristics of cement treated sand prepared by static compaction method", *Geomech. Eng*., **12**(6), 935-948. https://doi.org/10.12989/gae.2017.12.6.935.